

Measurement and Evaluation of Scatter Fractions for Digital Radiography with a Beam-Stop Array

Yu-Na Choi*[†], Hyo-Min Cho*[†], Yi-Seul Kim*, Su-Jung An*, Hee-Joung Kim*[†]

*Department of Radiological Science, College of Health Science,
[†]Research Institute of Health Science, Yonsei University, Wonju, Korea

Scatter radiation considerably affects radiographic image quality by reducing image contrast and contributing to a non-uniform background. Images containing a large portion of scatter radiation may result in an incorrect diagnosis. In the past few years, many efforts have been made to reduce the effects of scatter radiation on radiographic images. The purpose of this study is to accurately measure scatter fractions and evaluate the effectiveness of beam-stop arrays. To measure scatter fraction accurately, a beam-stop array and the SFC (Scatter Fraction Calculator) program were developed. Images were obtained using the beam-stop array for both an anti-scatter technique with an anti-scatter grid and an air gap technique. The scatter fractions of the images were measured using the SFC program. Scatter fractions obtained with an anti-scatter grid were evaluated and compared to scatter fractions obtained without an anti-scatter grid. Scatter fractions were also quantitatively measured and evaluated with an air gap technique. The effectiveness of the beam-stop array was demonstrated by quantifying scatter fractions under various conditions. The results showed that a beam-stop array and the SFC program can be used to accurately measure scatter fractions in radiographic images and can be applied for both developing scatter correction methods as well as systems.

Key Words: Scatter fraction, Beam-stop array, SFC program

INTRODUCTION

As an X-ray beam passes through a substance, five types of interactions can occur, including Compton effect, photoelectric effect, Raleigh scattering, pair production, and nuclear photoeffect. The Compton effect and Raleigh scattering result in the emission of scatter radiation, which causes many problems in radiography.^{1,2)} Scatter radiation can account for more than 90% of X-ray flux detected in the mediastinum region of chest radiographs and more than 70% on lung radiographs acquired without an anti-scatter grid.³⁾ This scatter radiation contributes to reducing contrast and causes image fog in clinical

radiographs. Because of these harmful effects of scatter radiation, it is important to find techniques for its reduction.⁴⁾

As a first step toward reducing scatter, one should carefully compress the object to be imaged and use tight collimation. However, especially in clinical situations, additional techniques for scatter reduction are still necessary. These may include the use of an anti-scatter grid, an air gap technique, or a slot technique,²⁾ the first two of which are the most common techniques for reducing scatter. The anti-scatter grid consists of a periodic array of radio-opaque foil strips (usually lead), separated by strips of radiolucent spacing material (typically paper or aluminum).⁵⁾ It can transmit the primary radiation, and also block scatter x-rays from all directions.⁵⁾ The air gap technique is based on the application of a certain distance, between the patient and the image recording system.²⁾ The reduction of the scatter at the image receptor with increasing distance from the patient's body has been described by various authors.⁶⁾

To improve image quality and reduce radiation exposure by reducing scatter radiation, we must accurately measure the scatter fraction, which is defined as the ratio of the intensity

This research sponsored by the Development Center of Mobile Emergency Medical Information System, Ministry of Health and Welfare (02-PJ3-PG6-EV08-0001).

Submitted November 3, 2009, Accepted December 17, 2009

Corresponding Author: Hee-Joung Kim, Department of Radiological Science, Institute of Health Science, Yonsei University, 234, Maeji-ri, Heungeop-myeon, Wonju 220-710, Korea

Tel: 033)760-2963, Fax: 033)760-2562

E-mail: hjk1@yonsei.ac.kr

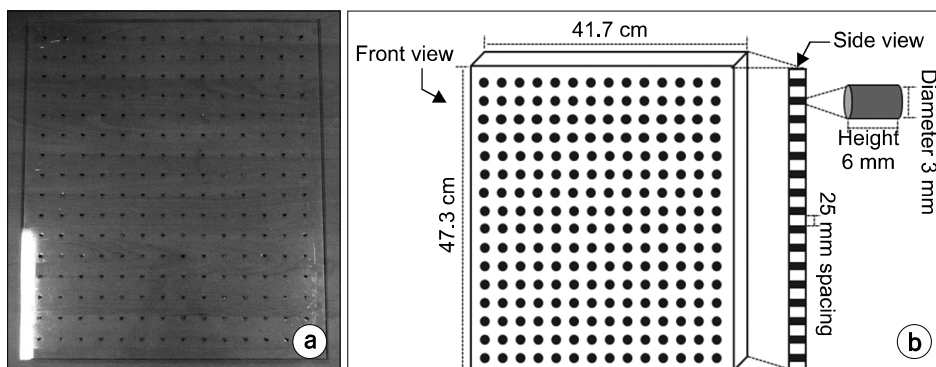


Fig. 1. (a) The photography of the beam-stop array. (b) Schematic diagram of the beam-stop array.

of the scatter radiation to that of the total radiation. Accurate evaluation of the scatter fraction requires an accurate estimation technique. We used a beam-stop array technique, which allows for scatter fraction measurements over various anatomic regions on radiographic images.

The goals of this study were to measure scatter fractions by developing an SFC (Scatter Fraction Calculator) program and to evaluate the effectiveness of the beam-stop array technique.

MATERIALS AND METHODS

1. Beam-stop array and FDA phantom

Scatter radiation measurements of a digital radiographic system were evaluated in terms of scatter fractions by using a beam-stop array and a geometric phantom.

To measure the scatter fractions, a beam-stop array was manufactured. The beam-stop array was constructed by 224 lead cylinders used as beam stops and 41.7×47.3 cm acrylic sheet. Each beam stop consisted of a 3 mm diameter and 6 mm height embedded in a 6 mm thickness sheet of acrylic. The intervals between the edges of each lead cylinder were 25 mm (Fig. 1).

The thickness (which represents more than 20 half-value layers: a transmission of 10^{-6} at diagnostic X-ray energies) of the beam-stop array effectively blocked all primary X-ray beams (Fig. 2).^{4,7)}

The phantom was manufactured based on a design by the Food and Drug Administration (FDA) for use in the Nationwide Evaluation of X-ray Trends (NEXT) program (Fig. 3a).

This FDA phantom, representing the chest of an average sized adult patient, was designed to assess the effects of at-

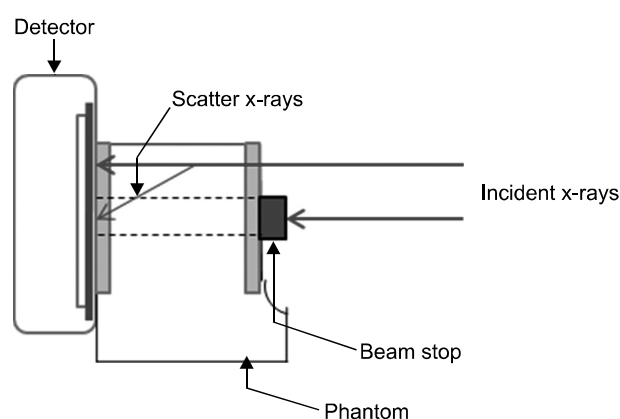


Fig. 2. Schematic diagram of photon trajectories for the beam-stop scatter measurement.

tenuation and scatter characteristics. The phantom includes blocks of acrylic, Lucite and aluminum. The geometry of the FDA phantom is shown in Fig. 3b.^{8,9)}

2. Imaging system

Images were acquired using a digital radiographic system. Table 1 lists the physical specifications of the imaging system.

3. Geometry and image acquisition

The distances from focus to detector and object were 180 cm and 153.3 cm, respectively. The beam-stop array was placed in front of the FDA phantom (Fig. 4, 5).

The uses of an anti-scatter grid and an air gap technique have been the most common techniques for reducing scatter radiation. The scatter fractions were measured using both of these techniques.

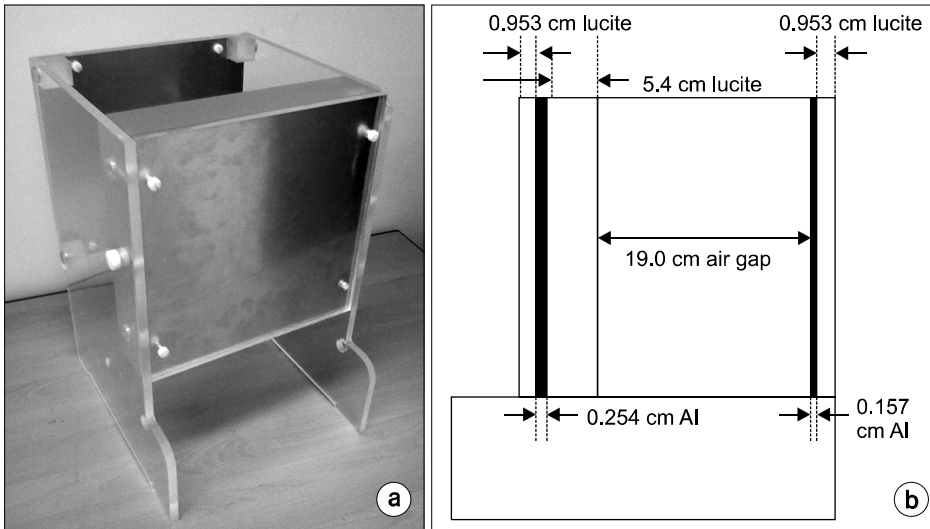


Fig. 3. (a) The manufactured FDA chest phantom. (b) Schematic diagram of the FDA phantom in side view. Al indicates aluminum.

Table 1. The physical specifications of the imaging system.

Characteristic	Value
Imaging system	TOSHIBA E7239X generator with a DRTECH FDXD-1417 detector
Capture element	Flat panel detector (direct conversion) TFT- amorphous selenium
Detecting area	356×427 mm
Image matrix size	2,560×3,072
Dynamic range	16,000 : 1
Image pixel size	0.139×0.139 mm
Filtration	1.8 mm Al
Focal spot size	2.0/1.0 mm

1) **Measurement of scatter fractions with and without an anti-scatter grid:** We measured scatter fractions both with and without an anti-scatter grid.^{8,9)} Exposures were made at 80 kV and 120 kV for an average sized adult chest. Fixed exposure factors were 320 mA, 0.01 sec exposure time and a distance of 180 cm from focus to detector. The anti-scatter grid had a density of 215 lines/inch and a ratio of 8:1 (Jungwon Precision Ind. Co., Ltd, South Korea).

2) **Measurement of scatter fractions using an air gap technique:** We measured the scatter fraction by increasing the air gap (increased from 0 to 5 cm with 1 cm spacing) without using an anti-scatter grid. Exposures were made at 80 kV, 320 mA and 0.01 sec exposure time. Fig. 5 shows the geometry for the scatter fraction measurement made by increasing the air gap.

4. Data analysis

A total of ten images were acquired in digital radiography. We used 16 bits to represent the intensity values of the image, making it possible to register 65,536 different gray levels. Images were obtained using a beam-stop array for both the anti-scatter grid and air gap techniques.

The scatter fraction is defined as the ratio of the intensity of scatter radiation to total radiation⁷⁾:

$$Scatter\ fraction = \frac{scatter\ (behind\ the\ beam\ stop)}{total\ (nonscatter + scatter)}$$

To calculate the scatter fraction, an SFC program was developed using MATLAB. The SFC program allowed extraction of mean ROI values behind the beam-stop shadow (the “scatter” value) and extracted the mean ROI values in between the beam-stops (“total” or “nonscatter+scatter” radiation). To reduce the error of mean ROI values, the region of interest (15×15 pixels) was set to exclude the pixels bordering the beam-stop edges.⁷⁾ Fig. 6 illustrates the ROI (15×15 pixels) behind the beam stop shadow in the radiographic images.

The mean value of scatter radiations at the range of 16 beam-stop arrays and total radiations at the range of 9 ROI (15×15 pixels) values were calculated (Fig. 7). This number of beam-stops was adequate to characterize the scatter fraction.¹⁰⁻¹³⁾ The blue circles on the Fig. 7 show the ROIs for measurement of mean gray value.

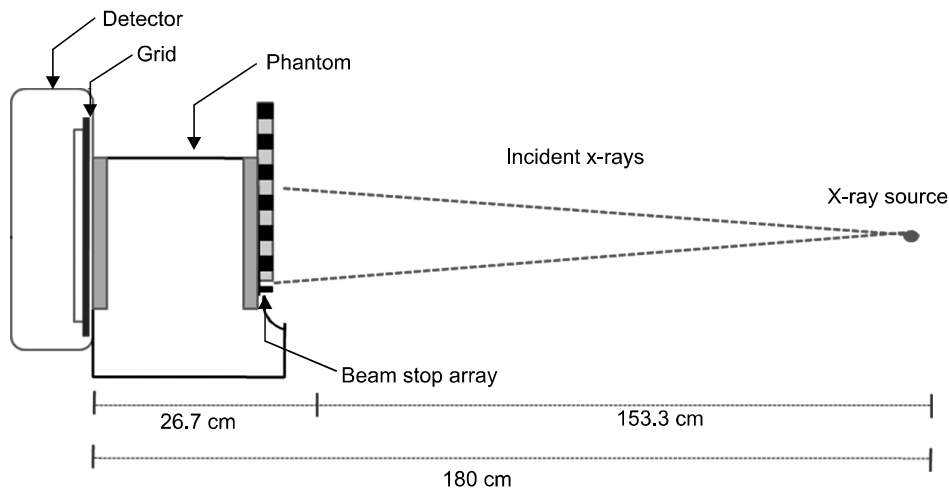


Fig. 4. Schematic diagram of the anti-scatter grid technique.

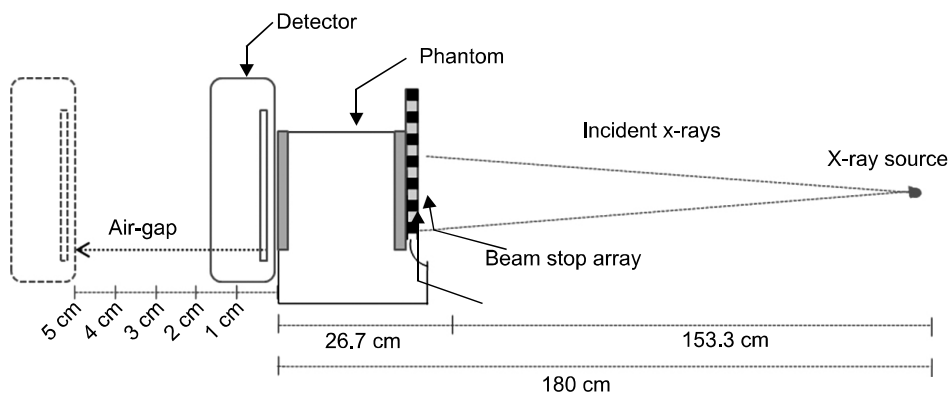


Fig. 5. Schematic diagram of the air-gap technique. The air-gap was increased from 0 to 5 cm with 1 cm spacing by moving the detector.

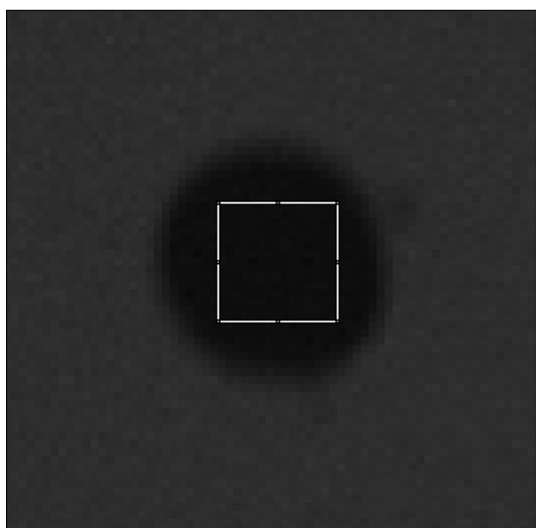


Fig. 6. ROI (15×15 pixels) behind the beam stop shadow. The area of a rectangular indicates the ROI for measurement of mean gray value.

For each beam-stop array image, the scatter fraction was then measured using the SFC program.

RESULTS

1. Measurement of scatter fractions with and without an anti-scatter grid

At 80 kVp and 120 kVp, the differences between the scatter fractions with and without the anti-scatter grid are shown in Table 2 and 3, respectively.

With the anti-scatter grid, scatter fractions were approximately 0.55 and 0.55 at 80 kVp and 120 kVp, respectively. Without the anti-scatter grid, the scatter fractions were approximately 0.71 and 0.71 at 80 kVp and 120 kVp, respectively.

The reference and experimental data at 80 kV and 120 kV without the anti-scatter grid were compared.²⁾

Fig. 8 shows a similarity between the reference and ex-

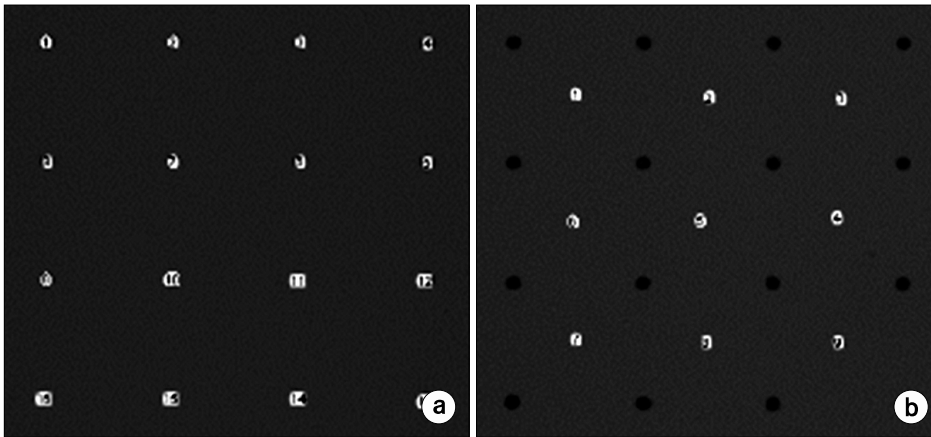


Fig. 7. (a) ROIs behind the beam stop (for the scatter value), (b) ROIs in between beam stops (for the "total," or "nonscatter+scatter," value).

Table 2. Scatter fractions with and without an anti-scatter grid at 80 kVp.

	Scatter radiation	Total radiation	Scatter fraction
	Mean pixel value of the ROI (m±SD)		
With	188±3.13	344±16.53	0.55
Without	582.7±22.55	815.6±31.45	0.71

Table 3. Scatter fractions with and without an anti-scatter grid at 120 kVp.

	Scatter radiation	Total radiation	Scatter fraction
	Mean pixel value of the ROI (m±SD)		
With	367±4.69	667±5.84	0.55
Without	1,053±32.32	1,484±46.89	0.71

Table 4. Scatter fractions using the air gap technique.

Air-gap (cm)	Scatter radiation	Total radiation	Scatter fraction
	Mean pixel value of the ROI (m±SD)		
0	579.0±11.23	815.6±8.78	0.71
1	524.7±17.32	812.4±13.01	0.65
2	470.4±26.33	780.8±33.87	0.60
3	432.6±12.95	764.2±31.60	0.57
4	419.0±7.97	748.0±4.65	0.56
5	400.4±16.98	725.2±28.55	0.55

perimental data. The scatter fraction depends on the X-ray tube voltage adapted from Reiss and Steinle 1973.²⁾

2. Measurement of scatter fractions using an air gap technique

Scatter fractions were measured using an air-gap technique in order to assess the usefulness of the beam-stop array and SFC program. Scatter fractions using the air-gap technique are shown in Table 4.

As for the beam-stop array technique, scatter fractions decreased as the air-gap distance between the phantom and the detector increases. This effect is shown in Fig. 9.

DISCUSSION AND CONCLUSION

In this study, the effectiveness of the beam-stop array technique and SFC program in measuring and evaluating the scatter effect in radiographic images was demonstrated. Scatter fractions measured using the beam-stop array and SFC pro-

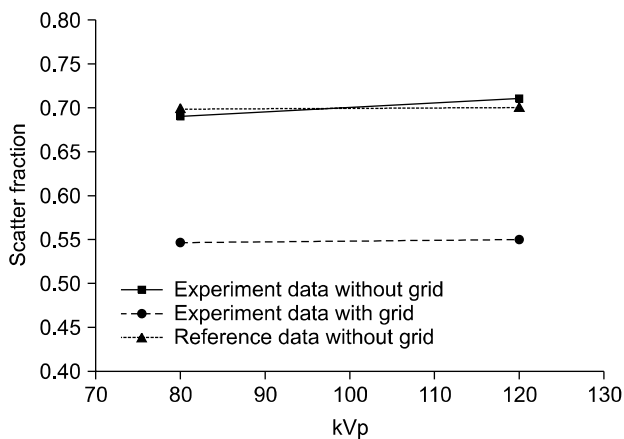


Fig. 8. Comparison of the reference data²⁾ with the experimental data.

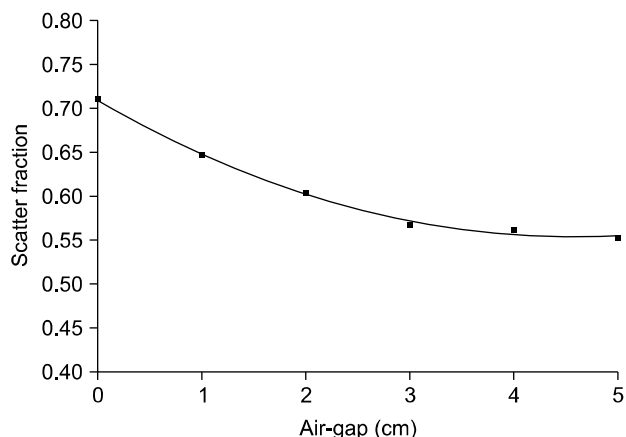


Fig. 9. Scatter fractions as a function of air gap size.

gram were in good agreement with previously reported values.²⁾

Scatter fractions are lower with the anti-scatter grid than without grid as shown in Table 2 and 3. Anti-scatter grids were able to reduce the scatter fraction to about 0.15 times. The scatter fraction with a 5 cm air-gap was approximately 0.16 times lower than the scatter fraction with a 0 cm air-gap, which suggests that air-gap techniques are useful for scatter reduction.

The beam-stop array technique together with the SFC program may help in the study of scatter characteristics in radiographic images. To get a reasonable signal on the detector, a suitable patient dose would be required and the system needs to be optimized.²⁾ Based on these results, measured scatter radiation and total radiation were lower at 80 kVp than at 120 kVp. In previous studies, a low kilovoltage was recommended for chest imaging with CR. This is consistent with clinical practices in the United Kingdom.⁸⁾ In order to demonstrate that 80 kVp without an anti-scatter grid gives suitable exposure,⁸⁾ scatter fractions need to be measured with varying mAs. Quantifying the exact scatter fraction may contribute to enhance the image quality and to develop both scatter correction

methods as well as systems.

REFERENCES

1. Kwon DG, Kwon DC, Kim HJ, et al: Medical Imaging Informatics. 1, Chungu, 2008, Seoul, pp. 123-143
2. Aichinger H, Dierker J, Joite-Barfu β S, et al: Radiation exposure and image quality in X-ray diagnostic. Radiology 1: 45-56 (2003)
3. Samei E, Lo JY, Yoshizizymi TT, et al: Comparative scatter and dose performance of slot-scan and full-field digital chest radiography Systems. Radiology 235:940-949 (2005)
4. Floyd CE, Baker JA, Lo JY, Ravin CE: Posterior beam-stop method for scatter fraction measurement in digital radiography. Investigate Radiology 27:119-123 (1992)
5. Tang CM, Stier E, Fischer K, Guckel H: Anti-scattering X-ray grid. Microsystem Technologies 4:187-192 (1998)
6. Sorenson JA, Floach J: Scatter rejection by air-gaps: an empirical model. Medical Physics 1:308-316 (1985)
7. Floyd CE, Lo JY, Chotas HG, Ravin CE: Quantitative scatter measurement in digital radiography using a photo-stimulable phosphor imaging system. Medical Physics 18: 408-413 (1991)
8. Ertan F, Mackenzie A, Urbanczyk HJ, Ranger NT, Samei E: Use of effective detective quantum efficiency to optimize radiographic exposures for chest imaging with computed radiography. The International Society for Optical Engineering, Bellingham, 2009, pp. 153-163
9. Samei E, Ranger NT, MacKenzie AM, et al: Detector or system? Extending the concept of detective quantum efficiency to characterize the performance of digital radiographic imaging systems. Radiology 249:926-937 (2008)
10. Chotas HG, Van Metter RL, Johnson GA, Ravin CE: Small object contrast in AMBER and conventional chest radiography. Radiology 180:853-859 (1991)
11. Jordan LK, Floyd CE, Lo JY, Ravin CE: Measurement of scatter fractions in erect posteroanterior and lateral chest radiography. Radiology 188:215-218 (1993)
12. Baydush AH, Ghem WC, Floyd CE: Anthropomorphic versus geometric chest phantoms: a comparison of scatter properties. Medical Physics 27:894-897 (2000)
13. Samei E, Saunders RS, Lo JY, et al: Fundamental imaging characteristics of a slot-scan digital chest radiographic system. Medical Physics 31:2687-2698 (2004)

Beam-Stop Array를 이용한 DR에서의 Scatter Fraction 측정 및 효용성 평가

*연세대학교 방사선학과, †연세대학교 보건과학연구소

최유나*[†] · 조호민*[†] · 김이슬* · 안수정* · 김희중*[†]

X-선 영상 촬영 시 피사체에 조사되는 X-선은 피사체 내부에서 필연적으로 산란을 일으킨다. 산란선은 영상시스템에 도달하여 영상의 대조도를 저하시키고 전체 농도(Background)를 불균일하게 만든다. 현재 학계의 연구 동향은 산란선에 의한 영상의 화질 저하를 방지하기 위한 방법 고안에 초점을 두고 있다. 본 연구의 목적은 영상에서의 scatter fraction을 정확하게 측정하여 영상시스템의 개선에 기여하고 대조도에 영향을 미치는 인자의 정량적 평가를 최적화하기 위함에 있다. Scatter fraction을 정확하게 측정하기 위하여 beam stop array를 제작하였다. 제작한 beam stop array를 이용하여 영상을 획득하고, 영상의 각 부위에서의 scatter fraction 측정을 자동화하기 위해 MATLAB을 이용한 프로그램(SFC: Scatter Fraction Calculator)을 개발하였다. 그리드 유·무와 air gap 효과에 따른 scatter fraction의 비교를 통하여 beam stop array와 SFC 프로그램의 효용성을 평가하였다. 그리드가 있을 경우의 scatter fraction이 그리드가 없는 경우에서 보다 낮은 값으로 측정되었으며 air gap이 증가함에 따라 scatter fraction이 감소함으로써 효용성을 입증했다. Beam stop array와 SFC 프로그램은 입증된 효용성을 기반으로 임상에서 흉부뿐 아니라 인체의 여러 부위에 이를 활용할 수 있을 것으로 기대된다.

중심단어: Beam stop array, Scatter fraction, SFC 프로그램